

# Sound Speeds, Cracking and Stability of Self-Gravitating Anisotropic Compact Objects

**H. Abreu**

*Centro de Física Fundamental,  
Departamento de Física, Facultad de Ciencias,  
Universidad de Los Andes, Mérida 5101, Venezuela y  
Centro Nacional de Cálculo Científico, Universidad de Los Andes, (CECALCULA),  
Corporación Parque Tecnológico de Mérida, Mérida 5101, Venezuela*

**H. Hernández**

*Laboratorio de Física Teórica,  
Departamento de Física, Facultad de Ciencias,  
Universidad de Los Andes, Mérida 5101, Venezuela*

and

**L. A. Núñez**

*Centro de Física Fundamental,  
Departamento de Física, Facultad de Ciencias,  
Universidad de Los Andes, Mérida 5101, Venezuela y  
Centro Nacional de Cálculo Científico, Universidad de Los Andes, (CECALCULA),  
Corporación Parque Tecnológico de Mérida, Mérida 5101, Venezuela*

November 26, 2024

## Abstract

Using the the concept of cracking we explore the influence of density fluctuations and local anisotropy have on the stability of local and non-local anisotropic matter configurations in general relativity. This concept, conceived to describe the behaviour of a fluid distribution just after its departure from equilibrium, provides an alternative approach to consider the stability of selfgravitating compact objects. We show that potentially unstable regions within a configuration can be identified as a function of the difference of propagations of sound along tangential and radial directions. In fact, it is found that these regions could occur when, at particular point within the distribution, the tangential speed of sound is greater than the radial one.

## 1 Introduction

An increasing amount of theoretical evidence strongly suggests that a variety of very interesting physical phenomena may take place giving rise to local anisotropy, i.e. unequal radial and tangential stresses  $P_r \neq P_\perp$  (see [1, 2], and references therein). In the newtonian regime it has been pointed out in the classical paper

by J.H. Jeans [3], and in the context of General Relativity, it was early remarked by G. Lemaître [4] that local anisotropy can relax the upper limits imposed on the maximum value of the surface gravitational potential. Since the pioneering work of R. Bowers and E. Liang [5] its influence in General Relativity has been extensively studied.

Any model for an anisotropic compact object is worthless if it is unstable against fluctuations of its physical variables and, different degrees of stability/instability will lead to different patterns of evolution in the collapse of self-gravitating objects. Therefore, as expected, stability of anisotropic matter configurations in General Relativity has been considered since the beginning of the effort to understand the effects of tangential pressures on a selfgravitating matter configuration [5]. Very soon, in 1976, W. Hillebrandt and K.O. Steinmetz [6], considering the problem of stability of fully relativistic anisotropic neutron star models, showed (numerically) that there exists a stability criterion similar to the one obtained for isotropic models. Later, Chan, Herrera and Santos [7] studied the role played by the local anisotropy in the onset of dynamical instabilities. They found that small anisotropies might drastically change the evolution of the system. Recently, an analytical method has been reported to extend the traditional Chandrasekhar's variational formalism [8] to anisotropic spheres [9].

L. Herrera introduces, in 1992, the concept of cracking (or overturning) [10] which is a qualitatively different approach to identify potentially unstable anisotropic matter configurations. The idea is that fluid elements, at both sides of the cracking point, are accelerated with respect to each other. It was conceived to describe the behaviour of a fluid distribution just after its departure from equilibrium. Later on, Herrera and collaborators [7] showed that even small deviations from local isotropy may lead to drastic changes in the evolution of the system as compared with the purely locally isotropic case. More over, they found that perturbations of density alone, do not take the system out of equilibrium for anisotropic matter configurations. Only perturbations of both, density and local anisotropy induce such departures [11,12]. This concept refers only to the tendency of the configuration to split (or to compress) at a particular point within the distribution but not to collapse or to expand. The cracking, overturning, expansion or collapse, has to be established from the integration of the full set of Einstein equations. Nevertheless, it should be clear that the occurrence of these phenomena could drastically alter the subsequent evolution of the system. If within a particular configuration no cracking (or overturning) is to appear, we could identify it as *potentially* stable (not absolutely stable), because other types of perturbations could lead to its expansions or collapse.

In the present paper we shall explore the influence that fluctuations of density and local anisotropy have on the possible cracking (or overturning) of local and non local anisotropic matter configurations in general relativity. We show that, for particular dependent perturbations, potentially unstable regions within anisotropic matter configurations could occur when the tangential speed of sound,  $\partial P_{\perp}/\partial\rho$ , is greater than the radial,  $\partial P_r/\partial\rho$ . This can give a more clear physical insight when considering the stability of particular anisotropic configurations when independent perturbations occurs.

This paper is organized as follows. Section 2 will describe our notation through a brief discussion of local anisotropy matter configurations. The concept of cracking for selfgravitating anisotropic matter configurations and its relation with the sound speeds, is considered in Section 3. The models and modeling strategy are presented in sections 4 and 5. Finally some results and conclusions are displayed in Section 6.

## 2 Anisotropic matter configuration in General Relativity

We shall consider a static spherically symmetric anisotropic distribution of matter, described by the Schwarzschild line element  $ds^2 = e^{\lambda(r)}dt^2 - e^{\nu(r)}dr^2 - r^2(d\theta^2 + \sin\theta d\phi^2)$  and having an energy-momentum tensor represented by  $\mathbf{T}_{\nu}^{\mu} = \text{diag} [\rho, -P_r, -P_{\perp}, -P_{\perp}]$ , where,  $\rho$  is the energy density,  $P_r$  the radial pressure and  $P_{\perp}$  the tangential pressure. For this matter configurations, the general relativistic hydrostatic equilibrium equation

can be written [5] as

$$\frac{dP_r}{dr} + (\rho + P_r) \left( \frac{m + 4\pi r^3 P_r}{r(r - 2m)} \right) - \frac{2}{r} (P_\perp - P_r) = 0. \quad (1)$$

Obviously, in the isotropic case ( $P_\perp = P_r$ ) it becomes the usual Tolman-Oppenheimer-Volkov (TOV) equation, which constrains the internal equilibrium structure of general relativistic, isotropic, static perfect fluid spheres and it is considered in standard textbooks of gravitation [13, 14],.

It is clear that the last term in 1,  $(P_\perp - P_r) \equiv \Delta$ , represents a “force” due to the local anisotropy. This “force” is directed outward when  $P_\perp > P_r \Leftrightarrow \Delta > 0$  and inward if  $P_\perp < P_r \Leftrightarrow \Delta < 0$ . Therefore we should have more massive configurations if  $\Delta > 0$  and less massive ones if  $\Delta < 0$ . This becomes more evident when the most extreme situations i.e.  $P_\perp \neq 0$  and  $P_r = 0$  or  $P_\perp = 0$  and  $P_r \neq 0$  are considered.

## 2.1 Ansätze for an anisotropic equation of state

If a density profile,  $\rho = \rho(r)$  is given, it is possible to integrate 1 when the definition of mass and the two other equations of state,

$$m(r) = 4\pi \int_0^r \rho \bar{r}^2 d\bar{r}, \quad P_r = P_r(\rho) \quad \text{and} \quad P_\perp = P_\perp(P_r), \quad (2)$$

are provided. The first equation of state,  $P_r = P_r(\rho)$ , corresponds to the standard barotropic equation of state for time-independent systems. In order to close the system, we have also to provide a second equation of state relating radial and tangential pressures,  $P_\perp = P_\perp(P_r)$ . It has been shown [15, 16], that there exists a unique global solution to (1) if:  $\rho$  is a continuous positive function;  $P_\perp(r)$  is a continuous differentiable function;  $P_r(r)$  is a solution to the equation with starting value  $P_\perp(0) = P_r(0)$ , and both pressures are positive at the center (i.e.  $P_\perp(0) = P_r(0) \geq 0$ ), therefore in the whole interior of the body.

Much of the efforts to disentangle the physics of very dense matter is reflected by the various “radial” equations of state:  $P_r = P_r(\rho)$  availables (see [17, 18] and references therein). In contrast, very little is known for the much less intuitive second equation of state  $P_\perp = P_\perp(P_r)$ . This is the reason why different ansätze are found to introduce anisotropy in matter configurations (see, for instance, references [1, 2, 5, 19, 20, 21, 22, 23, 24, 25, 26, 27, 28]). The unknown physics in the “tangential” equation of state is partially compensated by using heuristic criteria (geometric, simplicity or any other assumption relating radial and tangential pressures). Therefore, most of the exact solutions for the differential equation (1) found in the literature have been obtained from excessively simplifying heuristic assumptions and, in addition, some of the conditions to become “physically acceptable fluids” are not verified.

## 2.2 Acceptability conditions for anisotropic matter

The interior solution should satisfy some general physical requirements. Some of the “physical acceptability conditions” for anisotropic matter have been stated elsewhere [1, 2] as

1. density,  $\rho$ , radial pressure,  $P_r$ , and tangential pressure,  $P_\perp$ , should be positive everywhere inside the configuration.
2. gradients for density and radial pressure should be negative,

$$\frac{\partial \rho}{\partial r} \leq 0, \quad \text{and} \quad \frac{\partial P_r}{\partial r} \leq 0;$$

3. inside the static configuration the speed of sound should be less than the speed of light,

$$\frac{\partial P_r}{\partial \rho} \leq 1 \quad \text{and} \quad \frac{\partial P_\perp}{\partial \rho} \leq 1;$$

4. in addition to the above intuitive physical requirements, the interior solution should satisfy [29] either:
  - the *Strong Energy Condition*:  $\rho + P_r + 2P_\perp \geq 0$ ,  $\rho + P_r \geq 0$  and  $\rho + P_\perp \geq 0$  or
  - the *Dominant Energy Condition*:  $\rho \geq P_r$  and  $\rho \geq P_\perp$
5. junction conditions [30], match the matter configuration to the exterior Schwarzschild solution. Because of the continuity of the First Fundamental Form, the definition of mass in 2, evaluated at the boundary, becomes the total mass,  $M = m(a)$ , as measured by its external gravitational field. Moreover, the continuity of the Second Fundamental Form forces the radial pressure to vanish at the boundary,  $r = a$ , of the sphere  $P_r|_{r=a} = 0$ .

Notice that as a consequence of the junction conditions, the radial pressure should vanish at the boundary, but not the tangential one. However, both should be equal at the centre of the matter configuration. Also notice that there is no restriction on the gradient for the tangential pressure.

These reasonable physical requirements validate the assumptions made for both equations of state and, in many cases, exclude possible mathematical solutions of the system 1 and 2. Delgaty and Lake [31] considering the isotropic case ( $P_r = P_\perp$ ), found that, from 127 published solutions only 16 satisfy the above conditions. In particular, it is worth mentioning that, in order to have a causal theory of matter we have to demand that the sound speed be, at most, the speed of light. This important requirement when obviated, violates physical principles usually required for a matter physical theory [32].

### 3 Instability and cracking of anisotropic compact objects

As we have stressed above, in a series of papers Herrera and collaborators [10,11,12] elaborated the concept of cracking for selfgravitating isotropic and anisotropic matter configurations. It was introduced to describe the behaviour of fluid distributions just after its departure from equilibrium, when total non-vanishing radial forces of different signs appear within the system.

This section will describe the general framework of the cracking approach to identify potentially stable (and unstable) anisotropic matter configurations. We explicitly use some of the tacit assumptions for modeling cracking (or overturning) within these matter configurations and, finally, we propose a more intuitive criterion based on the difference of sound speeds to estimate the relative magnitude for the density and anisotropy perturbations and to evaluate the stability of bounded distributions.

#### 3.1 Cracking: the general framework

Herrera and collaborators state that there is cracking whenever the radial force is directed inward in the inner part of the sphere and reverses its sign beyond some value of the radial coordinate; or, when the force is directed outward in the inner part and changes sign in the outer part, we shall say that there is an overturning. These effects are related to the tidal accelerations of fluid elements [11,33], defined by

$$a^\alpha = \left[ -R_{\beta\gamma\mu}^\alpha u^\beta u^\mu + h_\beta^\alpha \left( \frac{du^\beta}{ds} \right)_{;\gamma} - \frac{du^\alpha}{ds} \frac{du_\gamma}{ds} \right] h_\nu^\gamma \delta x^\nu, \quad (3)$$

where  $\delta x^\nu$  is a vector connecting the two neighbouring particles;  $h_\beta^\alpha$  denotes the projector onto the three-space orthogonal to the four-velocity  $u^\alpha$  and  $du^\alpha/ds \equiv u^\mu u_{;\mu}^\alpha$ . Moreover, defining

$$R = \frac{dP_r}{dr} + (\rho + P_r) \left( \frac{m + 4\pi r^3 P_r}{r(r - 2m)} \right) - \frac{2}{r} \Delta, \quad (4)$$

it can be shown that 3 and 4, evaluated immediately after perturbation, lead to [11, 12]

$$R = -\frac{e^{\lambda}(\rho + P_r)}{e^{\nu/2}r^2} \int_0^a d\tilde{r} e^{\nu/2} \tilde{r}^2 \frac{d\Theta}{ds}, \quad (5)$$

where  $\Theta$  represents the expansion. Again, here,  $ds^2 = e^{\lambda(r)}dt^2 - e^{\nu(r)}dr^2 - r^2(d\theta^2 + \sin\theta d\phi^2)$ , the static Schwarzschild line element, has been assumed (see reference [11] for details). 4 is just the hydrostatic equilibrium equation 1 that vanishes for static (or slowly evolving) configurations. It can be appreciated from (5) that for cracking to occur at some value of  $0 \leq r \leq a$ , it is necessary that  $d\Theta/ds$  vanishes somewhere within the configuration. It is also clear the non local nature of this effect; and that small deviations from local isotropy may lead to drastic changes in the evolution of the system as compared with the purely locally isotropic case [12].

### 3.2 Cracking revisited

Following [12], we assume that the system having some pressure and density distributions satisfying  $R = 0$ , is perturbed from its hydrostatic equilibrium. Thus, fluctuations in density and anisotropy induce total radial forces ( $R \neq 0$ ) which, depending on their spatial distribution, may lead to the *cracking*; i.e radial force directed inward, ( $R > 0$ ), or, *overturning*, directed outward, ( $R < 0$ ) of the source. Therefore, we will be looking for a change of the sign of  $R$ , beyond some value of the radial coordinate. We will exclusively consider perturbations on both, density and local anisotropy, under which the system will be dynamically unstable. In other words,  $\delta\rho$  and  $\delta\Delta$  are going to be considered as independent perturbations; but fluctuations in mass and radial distribution pressure depend on density perturbations, i.e.

$$\rho + \delta\rho \Rightarrow \begin{cases} P_r(\rho + \delta\rho, r) \approx P_r(\rho, r) + \delta P_r \approx P_r(\rho, r) + \frac{\partial P_r}{\partial \rho} \delta\rho, \\ m(\rho + \delta\rho, r) = 4\pi \int_0^r (\rho + \delta\rho) \tilde{r}^2 d\tilde{r} \approx m(\rho, r) + \frac{4\pi}{3} r^3 \delta\rho. \end{cases} \quad (6)$$

Now on, expanding 4 we have, formally,

$$R \approx R_0(\rho, P_r, m, \Delta, r) + \underbrace{\frac{\partial R}{\partial \rho} \delta\rho + \frac{\partial R}{\partial P_r} \delta P_r + \frac{\partial R}{\partial m} \delta m + \frac{\partial R}{\partial \Delta} \delta\Delta}_{\tilde{R}} \quad (7)$$

and by using 6 it can be shown that

$$\tilde{R} = \delta\rho \left[ \left( 2 \frac{\partial R}{\partial \rho} + \frac{4\pi}{3} r^3 \frac{\partial R}{\partial m} \right) - \frac{2}{r} \frac{\delta\Delta}{\delta\rho} \right], \quad (8)$$

where

$$\frac{\partial R}{\partial \rho} = \frac{m + 4\pi P_r r^3}{r(r - 2m)} \geq 0 \quad \text{and} \quad \frac{\partial R}{\partial m} = \frac{(\rho + P_r)(1 + 8\pi P_r r^2)}{(r - 2m)^2} \geq 0. \quad (9)$$

It is immediately seen that, in order to have  $\tilde{R} = 0$  and consequently a change in its sign:

- both, the anisotropy and the density, have to be perturbed;
- both, anisotropy and density perturbations, have to have the same sign, i.e.  $\delta\Delta/\delta\rho > 0$ .

In order words, potentially stable configurations should have  $\delta\Delta/\delta\rho \leq 0$  everywhere because  $\tilde{R}$  never changes its sign [34].

### 3.3 Cracking and sound speeds

When arbitrary and independent density and anisotropy perturbations are considered (as in all previous works concerning cracking [10,11,12,34]) there is little physical criteria to establish the size (absolute and/or relative) of the perturbation, i.e. how small (or big) the perturbations should be. Different orders of magnitude (and relative size  $\delta\Delta/\delta\rho$ ) of perturbations could produce a cracking but we could be describing an unphysical scenario. Additionally, all these previous works only consider constant perturbations. It is possible that variable perturbations could be more efficient inducing cracking within a particular matter configuration. Again, there is no criteria in establishing the functionality of the perturbation throughout the matter distribution.

We are going to consider a particular type of dependent perturbation whose relative order of magnitude could be bounded by the behavior of some physical variables and could be checked by physical intuition. Obviously, general perturbations should be independent because they emerge from non related physical phenomena. But we are looking for some physical variables whose behavior could be checked in order to identify potential cracking.

It is easy to convince oneself that

$$\frac{\delta\Delta}{\delta\rho} \sim \frac{\delta(P_\perp - P_r)}{\delta\rho} \sim \frac{\delta P_\perp}{\delta\rho} - \frac{\delta P_r}{\delta\rho} \sim v_{s\perp}^2 - v_{sr}^2, \quad (10)$$

where  $v_{sr}^2$  and  $v_{s\perp}^2$  represent the radial and tangential sound speeds, respectively.

This will be the key concept, we will use in revisiting Herrera's approach to identify potentially unstable anisotropic matter configurations based on the concept of cracking. Now, by considering the sound speeds and evaluating 10, we could not only have a more precise idea of the relative order of magnitude of the perturbations ( $\delta\Delta$  and  $\delta\rho$ ) but also what are the regions more likely to be potentially unstable within a matter configuration.

It is clear that, because  $0 \leq v_{sr}^2 \leq 1$  and  $0 \leq v_{s\perp}^2 \leq 1$ , we have  $|v_{s\perp}^2 - v_{sr}^2| \leq 1$ . Thus,

$$-1 \leq v_{s\perp}^2 - v_{sr}^2 \leq 1 \Rightarrow \begin{cases} -1 \leq v_{s\perp}^2 - v_{sr}^2 \leq 0 & \text{Potentially stable,} \\ 0 < v_{s\perp}^2 - v_{sr}^2 \leq 1 & \text{Potentially unstable.} \end{cases} \quad (11)$$

Therefore, we can now evaluate potentially unstable regions within anisotropic models based on the difference of the propagation of sound within the matter configuration. Those regions where  $v_{sr}^2 > v_{s\perp}^2$  will be potentially unstable. On the other hand, if  $v_{sr}^2 \leq v_{s\perp}^2$  everywhere within a matter distribution, no cracking will occur. It is worth mentioning, concerning this criterion, one of the extreme matter configurations mentioned above ( $P_\perp \neq 0$  and  $P_r = 0$ ) is always potentially stable for cracking; and the other one ( $P_\perp = 0$  and  $P_r \neq 0$ ) becomes potentially unstable.

More over, for physically reasonable models, the magnitude of perturbations in anisotropy should always be smaller than those in density, i.e.  $|v_{s\perp}^2 - v_{sr}^2| \leq 1 \Rightarrow |\delta\Delta| \leq |\delta\rho|$ . When  $\delta\Delta/\delta\rho > 0$ , these perturbations lead to potentially unstable models.

Next section will be devoted to explore the effectiveness of this criterion on the stability of bounded matter configurations, having different equations of state. Again, we recall that the concept of cracking refers only to the tendency of the configuration to split and its occurrence has to be established from the integration of the full set of Einstein equations. In addition, it is clear that there could also be some perturbations that do not induce cracking but could cause instabilities that lead the configuration to collapse or to expand.

## 4 Perturbations and cracking for anisotropic configurations

In order to illustrate the workability of the above criterion 11, we shall work out several density profiles for models satisfying the physical acceptable conditions. Thus, in addition to the positivity of density and pressures profiles, their gradients and the fulfillment of the energy conditions (strong or dominant), we shall pay special and particular attention to the conditions bounding sound speeds (radial and tangential) within the matter configuration.

The idea will be to provide the density profile; then to obtain the radial pressure,  $P_r(r)$  from a “radial” equation of state  $P_r = P_r(\rho(r))$  and next to solve the tangential pressure  $P_\perp(r)$  from the anisotropic TOV 1. That is.

$$\rho(r) \rightarrow P_r = P_r(\rho(r)) \rightarrow P_\perp = P_r + \frac{r}{2} \frac{dP_r}{dr} + \frac{(\rho + P_r)}{2} \left( \frac{m + 4\pi r^3 P_r}{(r - 2m)} \right). \quad (12)$$

Then, the radial and tangential sound speeds are calculated and their difference  $|v_{s\perp}^2 - v_{sr}^2|$  is evaluated. Next, by using 11 the potential stability or unstability is established. This will be confirmed by a change in the sign of  $\tilde{R}$  described by 8 and 9.

To illustrate the above criterion 11 we shall analyze four cases concerning qualitatively different density profiles. We have selected two local (one singular and one non singular) and two non-local conformally flat anisotropic solutions. By *local models* we mean the standard way to express an equation of state where the energy density and radial pressure are related at a particular point within the configuration, i.e.  $P = P(\rho(r))$ . On the other hand, by *non local models* we will understand those where the radial pressure  $P_r(r)$  is not only a function of the energy density,  $\rho(r)$ , at that point; but also its functional throughout the rest of the configuration. Any change in the radial pressure takes into account the effects of the variations of the energy density within the entire volume [35, 27, 36]. It has been shown that in the static limit, this particular radial equation of state can be written as

$$P_r(r) = \rho(r) - \frac{2}{r^3} \int_0^r \bar{r}^2 \rho(\bar{r}) d\bar{r}. \quad (13)$$

It is clear that in equation (13) a collective behavior of the physical variables  $\rho(r)$  and  $P_r(r)$  is present.

### 4.1 Anisotropic Tolman VI model

This model was introduced by Cosenza, Herrera, Esculpi and Witten [20] starting from the singular Tolman VI density profile [37]. The original isotropic Tolman VI solution is not deprived of a physical meaning. It resembles a highly relativistic Fermi Gas with the corresponding adiabatic exponent of 4/3. By using a heuristic method these authors determine other physical variables representing an anisotropic static matter configuration; i.e.

$$\rho = \frac{K}{r^2}, \quad \Rightarrow P_r = \frac{3}{8\pi r^2} \left( \frac{1 - \sqrt{\frac{r}{a}}}{7 - 3\sqrt{\frac{r}{a}}} \right), \quad \Rightarrow P_\perp = \frac{3}{224\pi r^2} \left( \frac{21 - 25\sqrt{\frac{r}{a}}}{7 - 3\sqrt{\frac{r}{a}}} \right) \quad (14)$$

where, the junction conditions force the adjustment of the parameter, to  $K = 3/56\pi$ , and the radius is given by  $a = 81/49$ .

Sound speeds can be determined from 14, and can be written as

$$v_{sr}^2 = \frac{7(7 + 3\frac{r}{a} - 9\sqrt{\frac{r}{a}})}{(7 - 3\sqrt{\frac{r}{a}})^2} \quad \text{and} \quad v_{s\perp}^2 = \frac{3(49 + 25\frac{r}{a} - 70\sqrt{\frac{r}{a}})}{4(7 - 3\sqrt{\frac{r}{a}})^2}. \quad (15)$$

By using 14 the particular expresion for 8 can be obtained for this model as

$$\tilde{R}_{TolmanVI} = \frac{2\delta\rho}{r} \left[ \frac{(588 + 180\frac{r}{a} - 672\sqrt{\frac{r}{a}}) v_{s,r}^2 + 539 + 195\frac{r}{a} - 658\sqrt{\frac{r}{a}}}{16(7 - 3\sqrt{\frac{r}{a}})^2} - \frac{\delta\Delta}{\delta\rho} \right]. \quad (16)$$

It is worth mentioning that this model does not fulfill all the acceptability conditions stated in 2.2. It is singular at the center and near the boundary surface ( $r/a \simeq 0.706$ ) the tangential pressure becomes negative. Despite this unphysical situation, this model is presented because, as it will later become clear in Section 5, the difference in sound speed is constant through the whole configuration, which represents the above mentioned constant perturbation relation considered in previous works [10, 11, 12, 34].

## 4.2 Non local Stewart Model 1

This model emerges from a density profile proposed by B. W. Stewart [21], to describe anisotropic conformally flat static bounded configurations; which was also, recently, considered for non local anisotropic matter distributions [27]. Starting from this density profile we can find  $P_r(r)$  and  $P_\perp(r)$  as

$$\rho = \frac{1}{8\pi r^2} \frac{(e^{2Kr} - 1)(e^{4Kr} + 8Kr e^{2Kr} - 1)}{(e^{2Kr} + 1)^3} \quad (17)$$

$$P_r = \frac{1}{8\pi r^2} \frac{(1 - e^{2Kr})(e^{4Kr} - 8Kr e^{2Kr} - 1)}{(e^{2Kr} + 1)^3} \quad (18)$$

$$P_\perp = \frac{2K^2 e^{4Kr}}{\pi[1 + e^{2Kr}]^4}. \quad (19)$$

Again, the parameter  $K$  has to be obtained from the junction conditions; which means that  $K$  has to satisfy a trascendental equation

$$e^{4Ka} - 8Ka e^{2Ka} - 1 = 0 \quad \Rightarrow \quad K = \frac{1}{2a} \ln \left[ \frac{1 + (\frac{2M}{a})^{\frac{1}{2}}}{1 - (\frac{2M}{a})^{\frac{1}{2}}} \right]. \quad (20)$$

From 17, 18 and 19 the corresponding sound speeds can be found

$$v_{sr}^2 = \frac{8Kr e^{2Kr} [(e^{4Kr} - 1) + Kr [(e^{2Kr} - 2)^2 - 3]] - (e^{4Kr} - 1)^2}{(e^{4Kr} - 1)^2 + 8K^2 r^2 e^{2Kr} [(e^{2Kr} - 2)^2 - 3]} \quad (21)$$

and

$$v_{s\perp}^2 = \frac{32K^3 r^3 e^{4Kr} (e^{2Kr} - 1) (e^{2Kr} + 1)^{-1}}{(e^{4Kr} - 1)^2 + 8K^2 r^2 e^{2Kr} [(e^{2Kr} - 2)^2 - 3]}. \quad (22)$$

Now, equation 8 can also be obtained for this model as

$$\tilde{R}_{NLStewart1} = \frac{2\delta\rho}{r} \left[ \frac{[(e^{2Kr} + 1)(5 + v_{sr}^2) + 4Kr(e^{2Kr} - 1)] Kr}{6(e^{2Kr} + 1)^2 (e^{2Kr} - 1)^{-1}} - \frac{\delta\Delta}{\delta\rho} \right]. \quad (23)$$



### 4.3 Non local Stewart Model 2

This is a second density profile proposed by B. W. Stewart [21] which was recently proved to be non local [36] :

$$\rho = \frac{1}{8\pi r^2} \left[ 1 - \frac{\sin(2Kr)}{Kr} + \frac{\sin^2(Kr)}{K^2 r^2} \right] \quad (24)$$

$$P_r = -\frac{1}{8\pi r^2} \left[ 1 + \frac{\sin(2Kr)}{Kr} - 3 \frac{\sin^2(Kr)}{K^2 r^2} \right] \quad (25)$$

$$P_\perp = \frac{1}{8\pi r^2} \left[ 1 - \frac{\sin^2(Kr)}{K^2 r^2} \right]. \quad (26)$$

As in the previous models, junction conditions ( $M = m(a)$  and  $P_r(a) = 0$ ) determine the coupling constant  $K$ . In this case it has to satisfy also a trascendental equation

$$\frac{\sin Ka}{Ka} = \left( 1 - \frac{2M}{a} \right)^{1/2} \quad \text{and} \quad \cos Ka = \frac{1 - \frac{3M}{a}}{\sqrt{1 - \frac{2M}{a}}}. \quad (27)$$

Thus,

$$K = \frac{\sqrt{\frac{M}{a} \left( 4 - \frac{9M}{a} \right)}}{a - 2M}. \quad (28)$$

From 24, 25 and 26 the corresponding sound speeds can be found

$$v_{sr}^2 = \frac{\sin^2(Kr) (3 - K^2 r^2) - \frac{3}{2} \sin(2Kr) Kr}{[\cos(Kr) Kr - \sin(Kr)]^2} \quad \text{and} \quad v_{s\perp}^2 = \frac{\frac{Kr}{2} \left[ Kr + \frac{\sin(2Kr)}{2} \right] - \sin^2(Kr)}{[\cos(Kr) Kr - \sin(Kr)]^2}. \quad (29)$$

Now, equation 8 can also be obtained for this model as

$$\tilde{R}_{NLStewart2} = \frac{2\delta\rho}{r} \left[ \frac{2 \sin(2Kr) Kr - 9 \sin^2(Kr) (v_{sr}^2 + 1)}{12 \sin^4(Kr) [\sin(2Kr) Kr - 2 \sin^2(Kr)]^{-1}} - \frac{\delta\Delta}{\delta\rho} \right]. \quad (30)$$

### 4.4 Florides-Stewart-Gokhroo & Mehra Model

This density profile is due originally to P.S. Florides [38], but also corresponds to different solutions, considered by Stewart [21] and, more recently, by M. K. Gokhroo and A. L. Mehra [23]. The Florides-Stewart-Gokhroo-Mehra solution represents densities and pressures which, under particular circumstances [39], give rise to an equation of state similar to the Bethe-Börner-Sato newtonian equation of state for nuclear matter [33, 40, 41].

$$\rho = \rho = \rho_c \left(1 - \frac{Kr^2}{a^2}\right) \quad (31)$$

$$P_r = \frac{\rho_c}{j} \left(1 - \frac{2\mu r^2}{a^2} \left[\frac{5 - \frac{3Kr^2}{a^2}}{5 - 3K}\right]\right) \left(1 - \frac{r^2}{a^2}\right)^n, \quad (32)$$

$$P_\perp = P_r + \frac{\rho_c}{j} \left[ \frac{3\mu K}{5 - 3K} \eta^4 (1 - \eta^2)^n + \eta^2 \frac{e^\lambda}{2} \left[ \frac{15\mu e^{-2\lambda}}{j(5 - 3K)} (1 - \eta^2)^{2n} - 2\pi e^{-2\lambda} (1 - \eta^2)^{n-1} + \frac{5\mu j}{5 - 3K} \left(1 - \frac{3}{5} K \eta^2\right) (1 - K \eta^2) \right] \right], \quad (33)$$

with

$$\mu = \frac{M}{a}, \quad e^{-\lambda} = 1 - \frac{2\mu \eta^2 (5 - 3K \eta^2)}{5 - 3K} \quad \text{and} \quad \eta = \frac{r}{a}.$$

and  $\rho_c$  the density at the center of the matter configuration.

From 31, 32 and 33 the corresponding radial sound speed can be found as

$$v_{sr}^2 = \frac{2\mu (5 - 6K \eta^2) [1 - (1 + n) \eta^2] + n [5 - 3K (1 + 2\mu \eta^4)]}{K j (5 - 3K) (1 - \eta^2)^{1-n}} \quad (34)$$

and

$$v_{s\perp}^2 = v_{sr}^2 - \frac{1}{2jK\eta} \left[ \frac{6\mu K \eta^3 [2 - \eta^2(2 + n)]}{(5 - 3K)(1 - \eta^2)^{1-n}} + \frac{\eta}{e^{-\lambda}} \left[ \phi \left(1 - \frac{\eta \xi}{2e^{-\lambda}}\right) + \frac{\eta}{2} \Xi \right] \right], \quad (35)$$

where

$$\Xi = \frac{30\mu e^{-\lambda} (1 - \eta^2)^{2n}}{j(5 - 3K)} \left( \xi - \frac{2n\eta e^{-\lambda}}{1 - \eta^2} \right) - \frac{4\mu j K \eta (4 - 3K \eta^2)}{5 - 3K} - 4\pi e^{-\lambda} \left[ \xi - \frac{\eta e^{-\lambda}}{1 - \eta^2} \right] (1 - \eta^2)^{n-1} \quad (36)$$

$$\phi = \frac{1}{5 - 3K} \left[ (1 - \eta^2)^{2n} e^{-2\lambda} \left[ \frac{15\mu}{j} - \frac{2\pi (5 - 3K)}{(1 - \eta^2)^{n+1}} \right] + \frac{\mu j (5 - 3K \eta^2)}{(1 - K \eta^2)^{-1}} \right] \quad (37)$$

and

$$\xi = -\frac{4\mu \eta (5 - 6K \eta^2)}{5 - 3K}. \quad (38)$$

For this example equation 8 can also be obtained as

$$\begin{aligned} \tilde{R}_{FSGM} = & \frac{2\delta\rho}{r} \left[ \frac{2\mu v_{sr}^2}{(5 - 3K) j e^{-2\lambda} a \eta} \left[ \eta^2 [15e^{-\lambda} (1 - \eta^2)^n - j (5 - 6K \eta^2)] \right. \right. \\ & \left. \left. - \frac{2\mu (5 - 3K \eta^2) [15e^{-\lambda} (1 - \eta^2)^n + j (10 - 9K \eta^2)]}{5 - 3K} \right] \right. \\ & \left. - \frac{6\mu \eta^4}{(5 - 3K)^2 j^2} \left[ j^2 (9K^2 \eta^4 + 25) + 30j [e^{-\lambda} (1 - \eta^2) K - j] \eta^2 \right. \right. \\ & \left. \left. - 75e^{-2\lambda} (1 - \eta^2)^{2n} \right] - \frac{\delta\Delta}{\delta\rho} \right]. \end{aligned} \quad (39)$$

Density Profile	$M/a$	$M(M_\odot)$	$z_a$	$\rho_a \times 10^{14} (gr/cm^3)$	$\rho_c \times 10^{15} (gr/cm^3)$
<b>Tolman VI</b>	0.21	1.42	0.31	2.30	NA
<b>NL Stewart 1</b>	0.32	2.15	0.65	6.80	1.91
<b>NL Stewart 2</b>	0.39	2.68	1.19	8.49	2.14
<b>Gokhroo &amp; Mehra</b>	0.26	1.76	0.44	0.00	2.09

Table 1: All parameters have been chosen to represent a possible compact object with  $a = 10$  Km. and the corresponding mass function satisfying the physical acceptability and energy conditions

## 5 The modeling performed

As it can be appreciated from the parameters displayed in table 1, all the models considered have radius ( $a = 10$  Km.) and total masses,  $M$  (in terms of solar mass  $M_\odot$ ) that correspond to typical values for expected astrophysical compact objects. The boundary redshifts  $z_a$ , surface and central densities,  $\rho_a$  and  $\rho_c$  that emerge from our selection, also fit the typical values for these objects.

Profiles for the radial,  $v_{sr}^2$ , and tangential,  $v_{s\perp}^2$ , sound speeds, as well as its difference,  $v_{s\perp}^2 - v_{sr}^2$ , are displayed in Figure 1. The perturbation relation,  $\delta\Delta/\delta\rho \equiv v_{s\perp}^2 - v_{sr}^2$ , fulfills the physical restriction  $-1 \leq \delta\Delta/\delta\rho \leq 1$  for all models considered. Notice that  $\delta\Delta/\delta\rho$ , is constant within the matter distribution for the Tolman VI anisotropic model (plate *I* in Figure 1). This type of constant perturbation relations were standard for modeling cracking in previous works [10, 11, 12, 34]. Because  $\delta\Delta/\delta\rho < 0$ , the sound speed stability criterion, 11, states that in the Tolman VI anisotropic model, no cracking will occur. Non local Stewart models are sketched in plates *II* and *III*, respectively. For these two models we could implement variable perturbation relations,  $\delta\Delta/\delta\rho$ , through the matter configuration; because  $-1 \leq \delta\Delta/\delta\rho \leq 0$ , no cracking will occur in these models either. Finally, the most interesting scenario emerges from the Florides-Stewart-Gokhroo-Mehra model [23] with  $j = 7$ ,  $K = 1$  and  $n = 2$ , shown in plate *IV*. As it is evident from this plate, the perturbation relation,  $\delta\Delta/\delta\rho$  not only has a variable profile, but it also changes its sign, alternating potentially stable and unstable regions within the distribution. In fact, this model presents two potentially unstable regions:  $0 \lesssim \eta = r/a \lesssim 0.2570$  and  $0.7565 \lesssim \eta = r/a \lesssim 1$  where  $\delta\Delta/\delta\rho > 0$ .

The profiles of  $\tilde{R}$  for each model are plotted in Figure 2. and the above stability assumptions can be contrasted with the change in sign for the expressions 16, 23, 30 and 39. It is clear from the  $\tilde{R}$ -plots displayed in this figure, that the models of Tolman VI, NL Stewart 1 and NL Stewart 2 models do not present any cracking point (plates *I*, *II* and *III*, respectively). On the other hand, the Florides-Stewart-Gokhroo-Mehra model displays a cracking point at  $\eta \approx 0.17986$  within the first potentially unstable region,  $0 \lesssim \eta = r/a \lesssim 0.2570$ .

## 6 Results and conclusions

We have revisited the concept of cracking for selfgravitating anisotropic matter configurations introduced by L. Herrera and collaborators [10, 11, 12]. It has been shown that for some particular dependent perturbations, the ratio for fluctuations in anisotropy to energy density,  $\delta\Delta/\delta\rho$  can be interpreted in terms of the difference of sound speeds, i.e.  $\delta\Delta/\delta\rho \sim v_{s\perp}^2 - v_{sr}^2$ ; where  $v_{sr}^2$  and  $v_{s\perp}^2$  represent the radial and tangential sound speeds, respectively. It is evident from 11 that regions where  $v_{sr}^2 > v_{s\perp}^2$  will be potentially unstable. On the other hand, if  $v_{sr}^2 \leq v_{s\perp}^2$  everywhere within a matter distribution, no cracking will occur and it could be considered as stable.

This reinterpretation could be useful to refine and make the concept of cracking more physically related to the potential instability due to the behavior of some physical variables within matter configurations. It

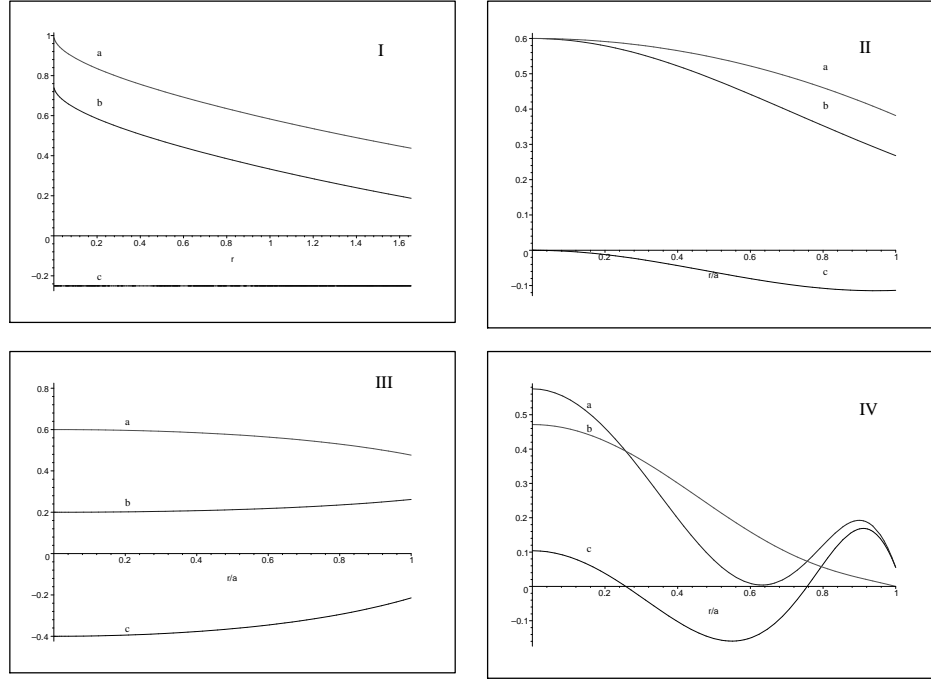


Figure 1: Variations of the radial and tangential sound speeds for anisotropic configurations. Plates *I*, *II*, *III* y *IV* represent Tolman VI, NL Stewart 1, NL Stewart 2 and Gokhroo & Mehra, respectively. Curves *a*, *b* and *c* correspond to  $v_{sr}^2$ ,  $v_s^2 \perp$  y  $v_s^2 \perp - v_{sr}^2$ , respectively.

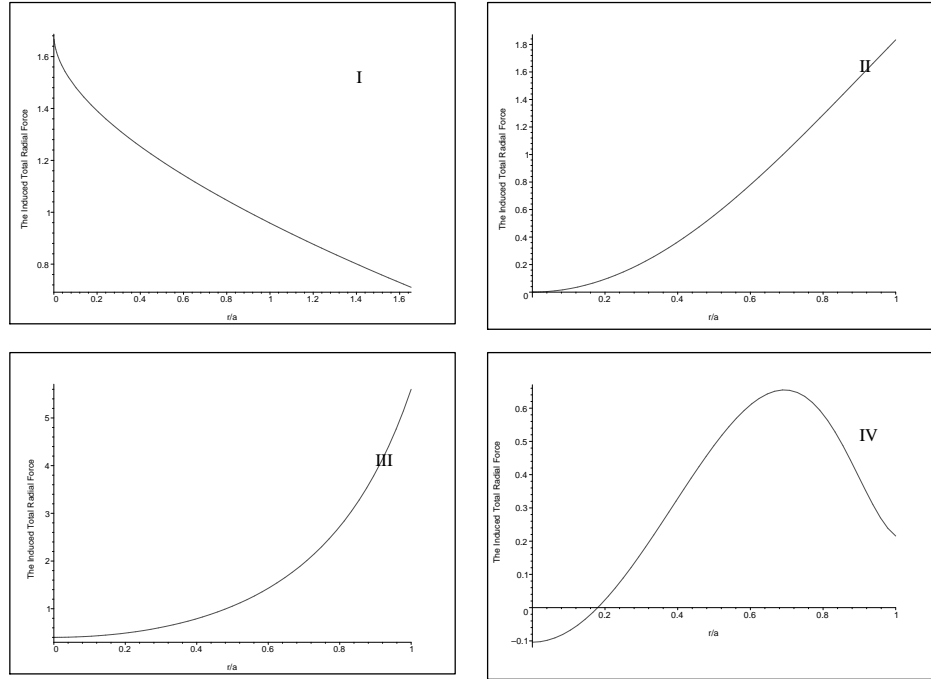


Figure 2: The induced total radial force  $\tilde{R}$  for the anisotropic configurations. Plots *I*, *II*, *III* and *IV* represent Tolman VI, NL Stewart 1, NL Stewart 2 and Gokhroo & Mehra, respectively.

is easy to determine each sound speed, their difference 10 and the sign of the difference. Thereafter, we could clearly identify from 8 which regions are more likely to be potentially unstable within a particular matter distribution. This can be appreciated from the Florides-Stewart-Gokhroo-Mehra model (Figure 2 plate IV) which displays a cracking point at  $\eta \approx 0.17986$  within the first potentially unstable region  $0 \lesssim \eta = r/a \lesssim 0.2570$ .

Additionally, because each sound speed has to be less than the speed of light, it implies that their difference has the physical restriction:  $|\delta\Delta/\delta\rho| \sim |v_{s\perp}^2 - v_{sr}^2| \leq 1$ . This is very important in order to characterize a particular model as potentially unstable. It is possible to find cracking points within a configuration for unphysical set of fluctuations in anisotropy and energy density, i.e.  $|\delta\Delta/\delta\rho| > 1$ , but the existence of these cracking points could not lead to physical potentially unstable models. More over, the physical restriction,  $|\delta\Delta/\delta\rho| \leq 1$  also conditions the relative order of magnitude of the perturbations.

The ratio of perturbations,  $\delta\Delta/\delta\rho$  are now not necessarily constant. Models considered in previous works [10, 11, 12, 34] have constant fluctuations, because there were no other criteria to introduce in order to evaluate the change in the sign of  $\tilde{R}$ . Now, the possibility to introduce variable fluctuations based on difference of sound speeds, enrich the applicability of the cracking framework to evaluate instabilities within anisotropic matter configurations.

It is worth mentioning that, concerning this criterion, one of the extreme matter configurations mentioned above  $P_\perp \neq 0$  and  $P_r = 0$  is always potentially stable, and the other  $P_\perp = 0$  and  $P_r \neq 0$  could experiment a cracking (or overturning) scenario. The study of matter configurations with vanishing radial stresses traces back to G. Lemaître [4] and for non static models have been considered in [1]. Recently, this model has been studied [42, 43] concerning its relation with naked singularities and conformally flat models has been considered in [24]. Extreme models with vanishing tangential stresses seems to be useful describing highly compact astrophysical objects having very large magnetic fields ( $B \gtrsim 10^{15}$  G) [44]

As we have pointed out, any model for a static compact object is worthless if it is unstable against fluctuations of its physical variables. If a particular static model is unstable against these fluctuations it could follow different possible patterns in its subsequent evolution. It could collapse, expand, split or overturn. Perturbations play a crucial role not only evaluating the stability of a particular static model, but identifying trends in possible future evolution of the model. Their study should be considered from different points of view and formalisms. In this work we have considered only those perturbations, related through radial and tangential sound speeds, that lead to identify potentially unstable regions. Independent perturbations (not related via any physical quantity) could also exist and could also lead to cracking (or overturning) points but, in this case there is no criteria to quantify their order of magnitude. Other types of perturbations leading to expanding or collapsing evolutions could be considered in the standard Chandrasekhar's variational formalism ( see [8,9] and references therein). Again, we stress the fact that those different possible evolution patterns for unstable configurations, refers only to a tendency. Its occurrence has to be established from the integration of the full set of Einstein equations.

## Acknowledgements

We are indebted to Luis Herrera Cometta for very fruitful discussions concerning the idea of cracking. We gratefully acknowledge the partial financial support of the Consejo de Desarrollo Científico Humanístico y Tecnológico de la Universidad de Los Andes (CDCHT-ULA) under project C-1009-00-05-A, and of the Fondo Nacional de Investigaciones Científicas y Tecnológicas (FONACIT) under projects S1-2000000820 and F-2002000426.

## References

- [1] Herrera L and Santos N O. Local anisotropy in self-gravitating systems. *Physics Reports*, 286(2):53–130, 1997.
- [2] Mak M K and Harko T. Anisotropic stars in general relativity. *Proc. Roy. Soc. Lond.*, A459:393–408, 2003.
- [3] Jeans J H. The motions of stars in a Kapteyn universe. *Monthly Notices of the Royal Astronomical Society*, 82:122–132, 1922.
- [4] Lemaitre G. L’univers en expansion. *Ann. Soc. Sci.(Bruxelles) A*, 53:51–85, 1933.
- [5] Bowers R L and Liang EPT. Anisotropic Spheres in General Relativity. *The Astrophysical Journal*, 188:657, 1974.
- [6] Hillebrandt W and Steinmetz K O. Anisotropic neutron star models-Stability against radial and non-radial pulsations. *Astronomy and Astrophysics*, 53(2), 1976.
- [7] Chan R, Herrera L, and Santos N O. Dynamical Instability for Radiating Anisotropic Collapse. *Royal Astronomical Society, Monthly Notices*, 265:533, 1993.
- [8] Chandrasekhar S. On stars, their evolution and their stability. *Rev. Mod. Phys.*, 56(2):137–147, Apr 1984.
- [9] Dev K and Gleiser M. Anisotropic Stars II: Stability. *General Relativity and Gravitation*, 35(8):1435–1457, 2003.
- [10] Herrera L. Cracking of self-gravitating compact objects. *Physics Letters A*, 165(206-210), 1992.
- [11] DiPrisco A., Fuenmayor E., Herrera L., and Varela V. Tidal forces and fragmentation of self-gravitating compact objects. *Physics Letters A*, 195:23 – 26, 1994.
- [12] DiPrisco A, Herrera L, and Varela V. Cracking of homogeneous self-gravitating compact objects induced by fluctuations of local anisotropy. *General Relativity and Gravitation*, 29(10):1239–1256, 1997.
- [13] Weinberg S. *Gravitation and Cosmology: Principles and Applications of the General Theory of Relativity*. Wiley, 1972.
- [14] Schutz B F. *A First Course in General Relativity*. Cambridge University Press, 1985.
- [15] Rendall A D and Schmidt B.G. Existence and properties of spherically symmetric static fluid bodies with a given equation of state. *Class. Quantum Grav*, 8:985–1000, 1991.
- [16] Mars M, Martín-Prats M M, and Senovilla J M M. Models of regular Schwarzschild black holes satisfying weak energy conditions. *Class. Quantum Grav*, 13:L51–L58, 1996.
- [17] Heiselberg H and Pandharipande V. Recent progress in neutron star theory. *Ann. Rev. Nucl. Part. Sci.*, 50:481–524, 2000.
- [18] Dany P and Reddy S. Dense matter in compact stars: Theoretical developments and observational constraints. *Ann. Rev. Nucl. Part. Sci.*, 56:327, 2006.
- [19] Heintzmann H and Hillebrandt W. Neutron stars with an anisotropic equation of state-Mass, redshift and stability. *Astronomy and Astrophysics*, 38(1), 1975.

- [20] Cosenza M, Herrera L, Esculpi M, and Witten L. Some models of anisotropic spheres in general relativity. *Journal of Mathematical Physics*, 22:118, 1981.
- [21] Stewart B W. Conformally flat, anisotropic spheres in general relativity. *J. Phys. A: Math. Gen.*, 15:2419–2427, 1982.
- [22] Rago H. Anisotropic spheres in general relativity. *Astrophysics and Space Science*, 183(2):333–338, 1991.
- [23] Gokhroo M K and Mehra A L. Anisotropic spheres with variable energy density in general relativity. *Gen. Rel. Grav.*, 26(1):75 – 84, 1994.
- [24] Herrera L, Di Prisco A, Ospino J, and Fuenmayor E. Conformally flat anisotropic spheres in general relativity. *J. Math. Phys.*, 42:2129–2143, 2001.
- [25] Herrera L., Martin J., and Ospino J. Anisotropic geodesic fluid spheres in general relativity. *J. Math. Phys.*, 43:4889–4897, 2002.
- [26] Dev K and Gleiser M. Anisotropic Stars: Exact Solutions. *General Relativity and Gravitation*, 34(11):1793–1818, 2002.
- [27] Hernández H. and Núñez L. A. Nonlocal equation of state in anisotropic static fluid spheres in general relativity. *Can. J. Phys.*, 82:29 – 51, 2004.
- [28] Chaisi M and Maharaj S D. Compact anisotropic spheres with prescribed energy density. *General Relativity and Gravitation*, 37(7):1177–1189, 2005.
- [29] Kolassis C, Santos N, and Tsoubelis D. Energy conditions for an imperfect fluid. *Classical and Quantum Gravity*, 5:1329–1338, 1988.
- [30] Bonnor W.B. and Vickers P.A. Junction conditions in general relativity. *General Relativity and Gravitation*, 13(1):29–36, 1981.
- [31] Delgaty MSR and Lake K. Physical acceptability of isolated, static, spherically symmetric, perfect fluid solutions of Einstein’s equations. *Comput. Phys. Commun.*, 115:395, 1998.
- [32] Ellis G, Maartens R, and MacCallum M. Causality and the speed of sound. *Preprint arXiv:gr-qc/0703121v1*, 2007.
- [33] Demianski M. *Relativistic Astrophysics*, volume 110 of *International Series in Natural Philosophy*. Pergamon Press, 1985.
- [34] Abreu H, Hernández H, and Núñez L A. Cracking of self-gravitating compact objects with a non local equation of state. *Journal of Physics: Conference Series*, 66:012038, 2007.
- [35] Hernández H., Núñez L. A., and Percoco U. Non-local equation of state in general relativistic radiating spheres. *Class. Quantum Grav.*, 16(3):871 – 896, 1998.
- [36] Muñoz A and Núñez L A. Soluciones conformemente planas con ecuación de estado no local. *Sup. Rev. Mex. de Física*, S52:112, 2006.
- [37] Tolman R C. Static Solutions of Einstein’s Field Equations for Spheres of Fluid. *Physical Review*, 55(4):364–373, 1939.
- [38] Florides P S. A new interior schwarzschild solution. *Proc. Roy. Soc. Lond*, A337:529 – 535, 1974.



- [39] Martínez J. Transport processes in the gravitational collapse of an anisotropic fluid. *Phys. Rev. D*, 53:6921 – 6940, 1996.
- [40] Shapiro S L and Teukolsky S A. *The Physics of Compact Objects*. Wiley, New York, 1983.
- [41] Bethe H A, Borner G, and Sato K. Nuclei in neutron matter. *Astr. and Astph*, 7:279 – 288, 1970.
- [42] Jhingan S and Magli G. Black holes versus naked singularities formation in collapsing einstein clusters. *Phys. Rev. D*, 61(12):124006, May 2000.
- [43] Barve S, Singh TP, and Witten L. Spherical Gravitational Collapse: Tangential Pressure and Related Equations of State. *General Relativity and Gravitation*, 32(4):697–717, 2000.
- [44] Chaichian M, Masood SS, Montonen C, Pérez Martínez A, and Pérez Rojas H. Quantum Magnetic Collapse. *Physical Review Letters*, 84(23):5261–5264, 2000.